Title
Compensation schemes and performance analysis of IQ imbalances in OFDM receivers

Journal
IEEE Transactions on Signal Processing, 53(8)

ISSN
1053-587X

Authors
Tarighat, Alireza
Bagheri, R
Sayed, A H

Publication Date
2005-08-01

Peer reviewed

Compensation Schemes and Performance Analysis of IQ Imbalances in OFDM Receivers

Alireza Tarighat, *Student Member, IEEE*, Rahim Bagheri, and Ali H. Sayed, *Fellow, IEEE*

***Abstract*—The implementation of orthogonal frequency division multiplexing (OFDM)-based physical layers suffers from the effect of In-phase and Quadrature-phase (IQ) imbalances in the front-end analog processing. The IQ imbalances can severely limit the achievable operating signal-to-noise ratio (SNR) at the receiver and, consequently, the supported constellation sizes and data rates. In this paper, the effect of IQ imbalances on OFDM receivers is studied, and system-level algorithms to compensate for the distortions are proposed. The algorithms include post-fast Fourier transform (FFT) least-squares and least mean squares (LMS) equalization, as well as pre-FFT correction using adaptive channel/distortion estimation and special pilot tones to enable accurate and fast training. Bounds on the achievable performance of the compensation algorithms are derived and evaluated as a function of the physical distortion parameters. A motivation is included for the physical causes of IQ imbalances and for the implications of the approach presented in this paper on designing and implementing wireless transceivers.**

***Index Terms*—Compensation algorithms for analog impairments, equalization, in-phase and quadrature-phase (IQ) imbalances, orthogonal frequency division multiplexing (OFDM).**

I. Introduction

ORTHOGONAL frquency division multiplexing (OFDM)-based physical layers have been selected for several wireless standards such as IEEE 802.11a, IEEE 802.11g, IEEE P802.15.3, IEEE 802.20, and IEEE 802.16 [1]–[5]. A low-cost implementation of such physical layers is challenging in view of impairments associated with the analog components. One such impairment is the imbalance between the I and Q branches when the received radio-frequency (RF) signal is down-converted to baseband. There are mainly two different receiver architectures to perform this down-conversion; one is the direct conversion RF receiver with its potential for low-cost and low-power implementation on silicon, and the other is the heterodyne receiver [6], [7]. A problem with direct conversion receivers when compared to heterodyne receivers is that the baseband signals are more severely distorted by imbalances within the I and Q branches [6], [7]. Moreover, such distortions are likely to increase in future systems when higher silicon integration is desired as well as higher carrier frequencies. This paper proposes baseband and digital signal processing techniques to compensate for such distortions in single-input single-output (SISO) OFDM receivers. The physical sources of IQ imbalances, the advantages of the approach taken in this paper for IQ compensation, and the implications of this approach on the implementation of wireless transceivers are motivated in Section II. The compensation of IQ imbalances in multi-input multi-output (MIMO) OFDM receivers is studied in the companion article [8].

The effect of IQ imbalances on SISO OFDM systems and the resulting performance degradation have been investigated in [9] and [10], and some useful compensation schemes have been reported in [11]–[13]. The contribution of the current paper is first to introduce a formulation that systematically describes the input–output relation in an OFDM system with IQ imbalances as a function of the channel taps and distortion parameters. The input–output relation is then used to motivate and derive new compensation algorithms (both pre-FFT and post-FFT-based), as well as an adaptive compensation algorithm with improved convergence rate. The proposed compensation schemes require training to estimate the distortion parameters that model the IQ imbalances. A special pilot tone pattern is proposed to simplify the training procedure. For systems such as IEEE 802.11a and IEEE 802.11g that feature a dedicated pilot sequence, the same training data used for channel estimation in standard OFDM systems could be used for joint channel and distortion estimation. For systems that do not provide dedicated training symbols, a decision-directed scheme can be used. Bounds on the performance of the compensation schemes are derived and evaluated for different IQ imbalance parameters using the input–output relations.

The paper is organized as follows. The next section explains the origin of the IQ problem and its impact on silicon implementation of wireless transceivers. It also motivates the approach of this paper. Section III describes the model used for IQ imbalances and formulates the effect of IQ imbalances on the received OFDM symbols. In Section IV, different algorithms for OFDM symbol estimation are proposed, which include post-FFT least-squares channel estimation and equalization, post-FFT adaptive equalization, distortion estimation, and pre-FFT correction using standard OFDM pilot symbols, as well as a special pilot pattern. Simulation results and performance comparison of different algorithms are given in Section V.

II. Motivation and Implications on System Implementation

The IQ imbalance compensation algorithms presented in this paper are valuable in eliminating one of the main barriers in de-

Manuscript received February 10, 2004; revised October 12, 2004. This work was supported in part by the National Science Foundation under Grants CCF-0208573 and ECS-0401188. A portion of this work appeared in the proceedings of IEEE International Conference on Acoustics, Speech, and Signal Processing, Montreal, QC, Canada, May 2004 [14]. The associate editor coordinating the review of this manuscript and approving it for publication was Dr. Petar M. Djuric.

The authors are with the Department of Electrical Engineering, University of California, Los Angeles, CA 90095 USA (e-mail: tarighat@ee.ucla.edu; bagheri@ee.ucla.edu; sayed@ee.ucla.edu).

Digital Object Identifier 10.1109/TSP.2005.851156

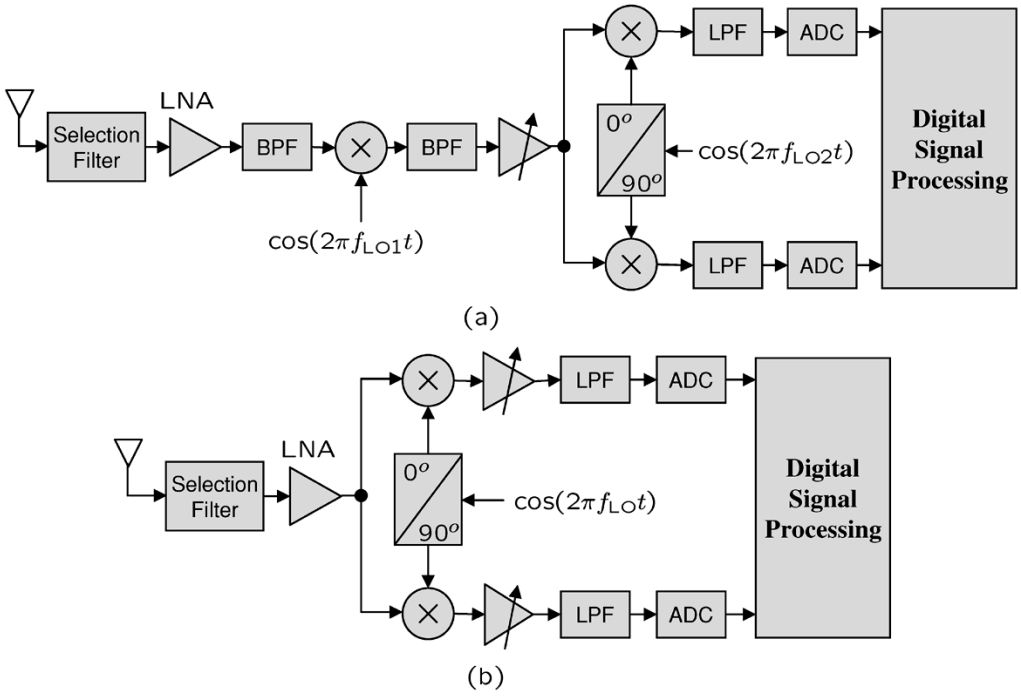

Fig. 1. Generic receiver architectures. (a) Heterodyne receiver with intermediate frequency (IF). (b) Zero intermediate frequency (ZIF) direct-conversion receiver.

signing the down-conversion stage in radio frequency receivers. This section explains the physical sources of IQ imbalances and the limitation of analog domain approaches to improve IQ matching and highlights the advantages of the digital signal processing solution proposed here.

Down-conversion is a fundamental stage in all radio frequency front-end architectures in which the high carrier frequency (f_{C}) signal is multiplied by local oscillating (LO) signals to be transferred to intermediate frequencies (f_{IF}) appropriate for further amplification and processing and, eventually, to the zero frequency (baseband). There are different architectures to convert the RF signal to the baseband, either through an intermediate frequency (IF) or by direct down-conversion to a baseband signal (zero intermediate frequency) [6]; see Fig. 1. There are advantages and disadvantages associated with each one [7]. Due to certain advantages in direct conversion (cost, area, power consumption, and less off-chip components), more of the future RF designs tend to be adopting this scheme, for instance, the OFDM-based IEEE802.11a system reported in [16]. Fig. 1 depicts these two architectures for the front-end implementation. Although IQ imbalances are an issue to be addressed for both of these architectures, addressing the imbalances in the analog domain is more severe and challenging in the zero intermediate frequency (ZIF) direct-conversion architecture. Therefore, the approach and techniques presented in this paper are of greater interest to ZIF direct-conversion architecture, although they can be adopted to the heterodyne architecture as well (the focus in this paper is on the direct-conversion architecture).

The down-conversion to the baseband in both architectures is implemented by what is known as complex down-conversion [7]; see Fig. 2. A complex down-converter basically multiplies the RF signal by the complex waveform $e^{-j2\pi f_{\mathrm{LO}}}$, where f_{LO} is the local oscillator frequency at the receiver. To perform the complex down-conversion, both the sine and cosine waveforms are required (known as in-phase and quadrature-phase LO). As seen in Fig. 2, in-phase LO, quadrature-phase LO, and two mixers (multipliers) are required to perform the complex down-conversion. Furthermore, the receiver is divided to I and Q branches (representing the real and imaginary parts of the equivalent baseband signal). Each branch is then followed by amplification, channel select filtering, and digitization. The key is that the effective sine and cosine waveforms at the receiver performing the down-conversion need to be orthogonal, i.e., exactly with 90° phase difference and with the same amplitude. Any mismatch between the processing performed on the I and Q branches after down-conversion will contribute to the overall IQ imbalance in the system and can significantly affect the performance of the system, as is shown in the simulation results.

Achieving such orthogonal waveforms at radio frequencies as high as 5.2 GHz (the band of operation for IEEE802.11a) is a challenging task for silicon implementation. Integrated circuit technologies such as low-cost complementary metal-oxide semiconductor (CMOS) technology have considerable mismatch between components due to fabrication process variations including doping concentration, oxide thickness, mobility, and geometrical sizes over the chip [17]. Since analog circuits are sensitive to the component variations, there will be unavoidable errors in the phases of LO and gains of IQ branches due to process mismatches and temperature variations.

In general, there are techniques developed in the analog domain to reduce such mismatches. Component mismatches are lowered by layout techniques and by increasing the physical size of the devices to benefit from the averaging over the area [17]. In addition, different circuit topologies have been used in analog circuit designs that are more robust to component

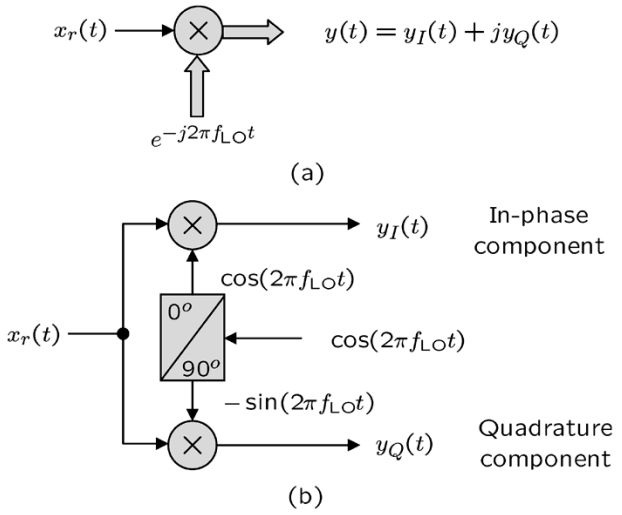

Fig. 2. Real signal mixed with a complex exponential for frequency down-conversion. (a) Arithmetic model. (b) Implementation.

mismatches. However, such techniques will increase the device sizes and raise the power consumption in the analog domain. Even accepting the power consumption penalty does not remove the mismatches completely. Any process variation in resistor or capacitor values causes them to introduce mismatches in the analog domain. Layout parasitic, dynamic fabrication, and temperature variations can limit the achievable match between the I and Q branches at high carrier frequencies [18].

The required specifications for systems such as IEEE 802.11a cannot be met purely based on analog domain techniques and without some type of adaptive compensation [16], [18]. Initially, compensation techniques were proposed in the analog domain to calibrate the IQ branches, but they suffer from different offsets, errors in the measurement feedback loop, and a long calibration process [18], and they do not meet the target performance requirements. The alternative approach is to estimate and compensate for such distortions in the digital domain by digital signal processing, as is done in this paper. There are major advantages associated with this technique. There is always a tradeoff in the analog domain between power, speed, and area for precision [6]. Such a tradeoff does not necessarily exist in the digital domain with the same intensity. The area and power consumption for digital processing scales down as the technology scales down, but the same trend does not hold for analog processing.

There are key issues to be considered regarding the imbalances. Perfect IQ matching *is not* possible in the analog domain, especially when low-cost fabrication technologies are used. Moreover, as the carrier frequencies increase, the imbalances become more severe and more challenging to eliminate. The increase in carrier frequencies will be the trend in the future communications systems to utilize more bandwidth. As higher data rates are targeted, higher constellation sizes are needed, and higher operating SNR are to be achieved to support such high density constellations. Higher SNR requirements translate to tougher IQ matching. On the other hand, adaptive techniques can be developed in the *digital domain* to track and eliminate imbalances. As will be shown in this paper, IQ distortion can be estimated and compensated along with the channel estimation and equalization procedure in the *digital* domain.

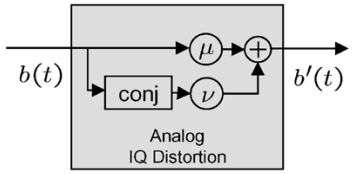

Fig. 3. Simplified model for analog IQ imbalances. In this model, the distortion parameters μ and ν are considered to be frequency independent.

III. Problem Formulation

Let $b(t)$ represent the received complex signal before being distorted by the IQ imbalance caused by analog processing. The distorted signal in the time domain can be modeled as [9], [10] (see Fig. 3)

$$b'(t) = \mu b(t) + \nu b^*(t). \tag{1}$$

The distortion parameters μ and ν are related to the amplitude and phase imbalances between the I and Q branches in the RF/Analog demodulation process through a simplified model as follows [10]:

$$\begin{aligned} \mu &= \cos(\theta/2) + j\alpha\sin(\theta/2) \\ \nu &= \alpha\cos(\theta/2) - j\sin(\theta/2) \end{aligned} \tag{2}$$

where θ and α are, respectively, the phase and amplitude imbalance between the I and Q branches. The phase imbalance is any phase deviation from the ideal 90^o between the I and Q branches. The amplitude imbalance is defined as

$$\alpha = \frac{a_I - a_Q}{a_I + a_Q}$$

where a_I and a_Q are the gain amplitudes on the I and Q branches. When stated in dB, the amplitude imbalance is computed as $10\log(1+\alpha)$. For instance, an amplitude imbalance of 0 dB corresponds to the ideal case of $\alpha = 0$. The values of θ and α are not known at the receiver since they are caused by manufacturing inaccuracies in the analog components.

The effect of IQ imbalances on an OFDM system and the resulting distortion on the received OFDM signal have been discussed in [11]–[13]. A derivation of the OFDM signals in the presence of IQ imbalances using the formulation of [14] is presented below. This formulation will be used to motivate and evaluate several baseband compensation techniques.

In OFDM systems, a block of data is transmitted as an OFDM symbol. Assuming a symbol size equal to N (where N is a power of 2), the transmitted block of data is denoted by

$$\mathbf{s} \triangleq [\mathbf{s}(1) \quad \mathbf{s}(2) \quad \dots \quad \mathbf{s}(N)]^{\mathrm{T}} \tag{3}$$

where $[\cdot]^{\mathrm{T}}$ is the transposition operation. Each block is passed through the IDFT operation:

$$\bar{\mathbf{s}} = \mathbf{F}^*\mathbf{s} \tag{4}$$

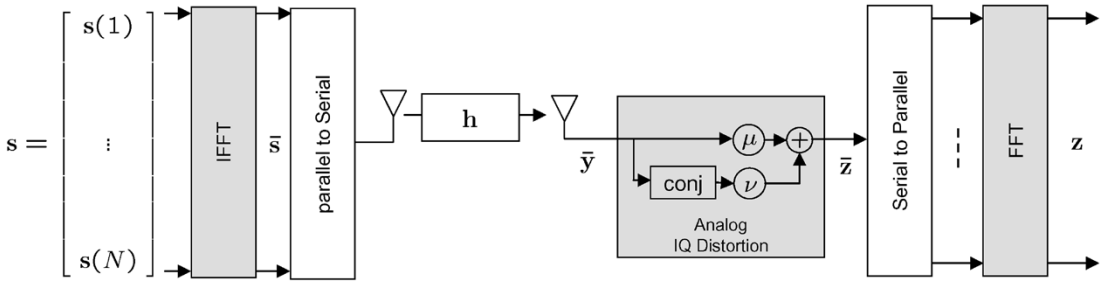

Fig. 4. Block diagram representation of an OFDM system with IQ imbalances.

where $\mathbf{F}$ is the unitary discrete Fourier transform (DFT) matrix of size N defined by

$$[\mathbf{F}]_{ik} \triangleq \frac{1}{\sqrt{N}} e^{\frac{-j2\pi ik}{N}} \quad j = \sqrt{-1} \qquad i,k = \{0,1,\ldots,N-1\}.$$

A cyclic prefix of length P is added to each transformed block of data and then transmitted through the channel. A finite impulse response (FIR) model with $L+1$ taps is assumed for the channel, i.e.,

$$\mathbf{h} = [h_0 \quad h_1 \quad \ldots \quad h_L]^{\mathrm{T}} \tag{5}$$

with $L \leq P$ in order to preserve the orthogonality between tones. At the receiver, the received samples corresponding to the transmitted block $\bar{\mathbf{s}}$ are collected into a vector, after discarding the received cyclic prefix samples. The received block of data before being distorted by IQ imbalances can be written as [15]

$$\bar{\mathbf{y}} = \mathbf{H}^c \bar{\mathbf{s}} + \bar{\mathbf{v}} \tag{6}$$

where

$$\mathbf{H}^c = \begin{bmatrix} h_0 & h_1 & \cdots & h_L & & & \\ & h_0 & h_1 & \cdots & h_L & & \\ & & \ddots & & & \ddots & \\ & & & h_0 & h_1 & \cdots & h_L \\ \vdots & & & & \ddots & & \vdots \\ h_2 & \cdots h_L & & & & h_0 & h_1 \\ h_1 & \cdots & h_L & & & & h_0 \end{bmatrix} \tag{7}$$

is an $N \times N$ circulant matrix, and $\bar{\mathbf{v}}$ is additive white noise at the receiver. It is known that $\mathbf{H}^c$ can be diagonalized by the DFT matrix as $\mathbf{H}^c = \mathbf{F}^* \mathbf{\Lambda} \mathbf{F}$, where

$$\mathbf{\Lambda} = \mathrm{diag}\{\lambda\} \tag{8}$$

and the vector λ is related to $\mathbf{h}$ via

$$\lambda = \sqrt{N}\mathbf{F}^* \begin{bmatrix} \mathbf{h} \\ \mathbf{0}_{(N-(L+1))\times 1} \end{bmatrix} \tag{9}$$

Then, (6) gives

$$\bar{\mathbf{y}} = \mathbf{F}^* \mathbf{\Lambda} \mathbf{F} \bar{\mathbf{s}} + \bar{\mathbf{v}} = \mathbf{F}^* \mathrm{diag}(\lambda) \mathbf{F} \bar{\mathbf{s}} + \bar{\mathbf{v}}. \tag{10}$$

The received block of data $\bar{\mathbf{y}}$ after being distorted by IQ imbalances is given by

$$\bar{\mathbf{z}} = \mu \bar{\mathbf{y}} + \nu \mathrm{conj}(\bar{\mathbf{y}}) \tag{11}$$

where the notation $\mathrm{conj}(\bar{\mathbf{y}})$ denotes a column vector whose entries are the complex conjugates of the entries of $\bar{\mathbf{y}}$; see Fig. 4. Now, remember that the DFT of the complex conjugate of a sequence is related to the DFT of the original sequence through a mirrored relation (assuming $1 \leq n \leq N$ and $1 \leq k \leq N$):

$$\begin{aligned} x(n) &\xrightarrow{\mathrm{DFT}} X(k) \\ x^*(n) &\xrightarrow{\mathrm{DFT}} X^*(N-k+2). \end{aligned} \tag{12}$$

For notational simplicity, we denote this operation by the superscript #, i.e., for a vector X of size N, we write

$$X = \begin{bmatrix} X(1) \\ X(2) \\ \vdots \\ X(N/2) \\ X(N/2+1) \\ X(N/2+2) \\ \vdots \\ X(N) \end{bmatrix} \Longrightarrow X^{\#} = \begin{bmatrix} X^*(1) \\ X^*(N) \\ \vdots \\ X^*(N/2+2) \\ X^*(N/2+1) \\ X^*(N/2) \\ \vdots \\ X^*(2) \end{bmatrix}. \tag{13}$$

Thus, if

$$X = \mathbf{F}x \quad \text{then} \quad X^{\#} = \mathbf{F}\mathrm{conj}(x). \tag{14}$$

Now, from (6), we have

$$\mathrm{conj}(\bar{\mathbf{y}}) = \mathrm{conj}(\mathbf{H}_c)\mathrm{conj}(\bar{\mathbf{s}}) + \mathrm{conj}(\bar{\mathbf{v}}) \tag{15}$$

where $\mathrm{conj}(\mathbf{H}_c)$ is a circulant matrix defined in terms of $\mathrm{conj}(\mathbf{h})$, as in (7). Moreover

$$\sqrt{N}\mathbf{F}^* \begin{bmatrix} \mathrm{conj}(\mathbf{h}) \\ \mathbf{0}_{(N-(L+1))\times 1} \end{bmatrix} = \lambda^{\#} \tag{16}$$

and

$$\mathrm{conj}(\mathbf{H}_c) = \mathbf{F}^* \mathrm{diag}(\lambda^{\#}) \mathbf{F}. \tag{17}$$

Substituting the above into (15) results in

$$\mathrm{conj}(\bar{\mathbf{y}}) = \mathbf{F}^* \mathrm{diag}(\lambda^{\#}) \mathbf{s}^{\#} + \mathrm{conj}(\bar{\mathbf{v}}). \tag{18}$$

Let us now consider a receiver that applies the DFT operation to the received block of data, as is done in a standard OFDM

receiver. Applying the DFT matrix to (11), i.e., setting $\mathbf{z} = \mathbf{F}\bar{\mathbf{z}}$, and substituting (10) and (18) into (11) lead to

$$\mathbf{z} = \mu \text{diag}(\lambda)\mathbf{s} + \nu \text{diag}(\lambda^{\#})\mathbf{s}^{\#} + \mathbf{v} \tag{19}$$

where $\mathbf{v}$ is a transformed version of the original noise vector $\bar{\mathbf{v}}$. As seen from (19), the vector $\mathbf{z}$ is no longer related to the transmitted block $\mathbf{s}$ through a diagonal matrix, as is the case in an OFDM system with ideal I and Q branches. For simplicity of presentation, we discard the samples corresponding to tones 1 and $N/2+1$, i.e., $\mathbf{z}(1)$ and $\mathbf{z}(N/2+1)$,[1] and define two new vectors

$$\begin{aligned}\tilde{\mathbf{s}} &= \text{col}\{\mathbf{s}(2), \ldots, \mathbf{s}(N/2), \mathbf{s}^*(N/2+2), \ldots, \mathbf{s}^*(N)\} \\ \tilde{\mathbf{z}} &= \text{col}\{\mathbf{z}(2), \ldots, \mathbf{z}(N/2), \mathbf{z}^*(N/2+2), \ldots, \mathbf{z}^*(N)\}.\end{aligned} \tag{20}$$

The second-half elements in $\tilde{\mathbf{s}}$ and $\tilde{\mathbf{z}}$ are conjugated due to the structure of (19). The reason for discarding the two samples is that the transformation (13) returns the same indices only for $k = 1$ and $k = N/2+1$ and mirrors and conjugates all other tones. In other words, in (13), $X(1)$ and $X(N/2+1)$ become $X^*(1)$ and $X^*(N/2+1)$, respectively, without any change in their indices. For all other tones, their indices become mirrored around the tone $N/2+1$. In order to have a unified formulation for all the tones, these two tones are discarded. However, if desired, a set of equations can be derived specifically for the tones 1 and $N/2+1$ in a similar manner to (22)–(24) below. Using (20), (19) leads to (21), shown at the bottom of the page, where $\tilde{\mathbf{v}}$ is related to $\mathbf{v}$ in a manner similar to (20). Note that the matrix $\tilde{\mathbf{\Lambda}}$ in the above equation is not a diagonal matrix, as is the case for $\mathbf{\Lambda}$ in (10), although it collapses to a diagonal matrix by setting ν equal to zero. Equation (21) can be reduced to 2×2 decoupled subequations, for $k = \{2, \ldots, N/2\}$, where each is written as

$$\mathbf{z}_k = \mathbf{\Gamma}_k \mathbf{s}_k + \mathbf{v}_k \tag{22}$$

where

$$\mathbf{z}_k = \begin{bmatrix} \mathbf{z}(k) \\ \mathbf{z}^*(N-k+2) \end{bmatrix}$$

$$\mathbf{s}_k = \begin{bmatrix} \mathbf{s}(k) \\ \mathbf{s}^*(N-k+2) \end{bmatrix} \tag{23}$$

$$\mathbf{\Gamma}_k = \begin{bmatrix} \mu\lambda(k) & \nu\lambda^*(N-k+2) \\ \nu^*\lambda(k) & \mu^*\lambda^*(N-k+2) \end{bmatrix} \tag{24}$$

[1]Note that in standardized OFDM systems such as IEEE 802.11a [1], these two tones do not carry any information due to implementation issues. Sending zeros on these two tones relaxes the implementation requirements on the receiver analog filters and DC offset.

and $\mathbf{v}_k$ is the corresponding noise on tone k defined from the noise vector $\mathbf{v}$ in a manner similar to (23). The objective is to recover $\mathbf{s}_k$ from $\mathbf{z}_k$ in (22) for $k = \{2, \ldots, N/2\}$, or, equivalently, $\tilde{\mathbf{s}}$ from $\tilde{\mathbf{z}}$ in (21).

IV. Proposed Compensation Algorithms

The estimation problem posed by (22)–(24) can be solved by different approaches.

A. Least-Squares Equalization

The least-squares estimate of $\mathbf{s}_k, k = \{2, \ldots, N/2\}$, which is denoted by $\hat{\mathbf{s}}_k$, is given by [19]:

$$\hat{\mathbf{s}}_k = (\delta \mathbf{I}_2 + \mathbf{\Gamma}_k^* \mathbf{\Gamma}_k)^{-1} \mathbf{\Gamma}_k^* \mathbf{z}_k. \tag{25}$$

where a regularization parameter $\delta > 0$ could be used when it is desired to combat ill-conditioning in the data $\mathbf{\Gamma}_k$. In order to implement the solution (25), the channel information (λ) and the distortion parameters (μ, ν) are required. Training symbols are required to enable the receiver to estimate those values. Thus, note that we may use (22) for channel estimation by rewriting it as

$$\mathbf{z}_k = \begin{bmatrix} \mathbf{s}(k) & 0 & \mathbf{s}^*(N-k+2) & 0 \\ 0 & \mathbf{s}(k) & 0 & \mathbf{s}^*(N-k+2 \end{bmatrix} \times \begin{bmatrix} \mu\lambda(k) \\ \nu^*\lambda(k) \\ \nu\lambda^*(N-k+2) \\ \mu^*\lambda^*(N-k+2) \end{bmatrix} + \mathbf{v}_k. \tag{26}$$

Assuming n_{Tr} OFDM symbols are transmitted for training, then n_{Tr} realizations of the above equation can be collected to perform the least-squares estimation of the elements forming $\mathbf{\Gamma}_k$, i.e., the channel taps $\{\lambda(k), \lambda^*(N-k+2)\}$ and the distortion parameters $\{\mu, \nu\}$. The estimated $\mathbf{\Gamma}_k$ can then be substituted into (25) for data estimation. The same training data used for channel estimation in standard OFDM systems such as IEEE802.11a and IEEE802.11g can be used in this scheme as the training symbols for joint channel and distortion estimation. For systems that do not provide dedicated training symbols, the following can be done. A decision-directed scheme can be used where the recovered data at the receiver are reused for training. In this case, a low density constellation [e.g., quadrature phase shift keying (QPSK)] can be used during the initial transmission phase since errors due to IQ imbalances are less severe for low density constellations.

The estimator (25) is optimal in the least-squares sense and will be referred to as post-FFT least-squares equalization. A

$$\tilde{\mathbf{z}} = \underbrace{\begin{bmatrix} \mu\lambda(2) & & & & & & \nu\lambda^*(N) \\ & \ddots & & & & \iddots & \\ & & \mu\lambda(N/2) & \nu\lambda^*(N/2+2) & & & \\ & & \nu^*\lambda(N/2) & \mu^*\lambda^*(N/2+2) & & & \\ & \iddots & & & & \ddots & \\ \nu^*\lambda(2) & & & & & & \mu^*\lambda^*(N) \end{bmatrix}}_{\tilde{\mathbf{\Lambda}}} \tilde{\mathbf{s}} + \tilde{\mathbf{v}} \tag{21}$$

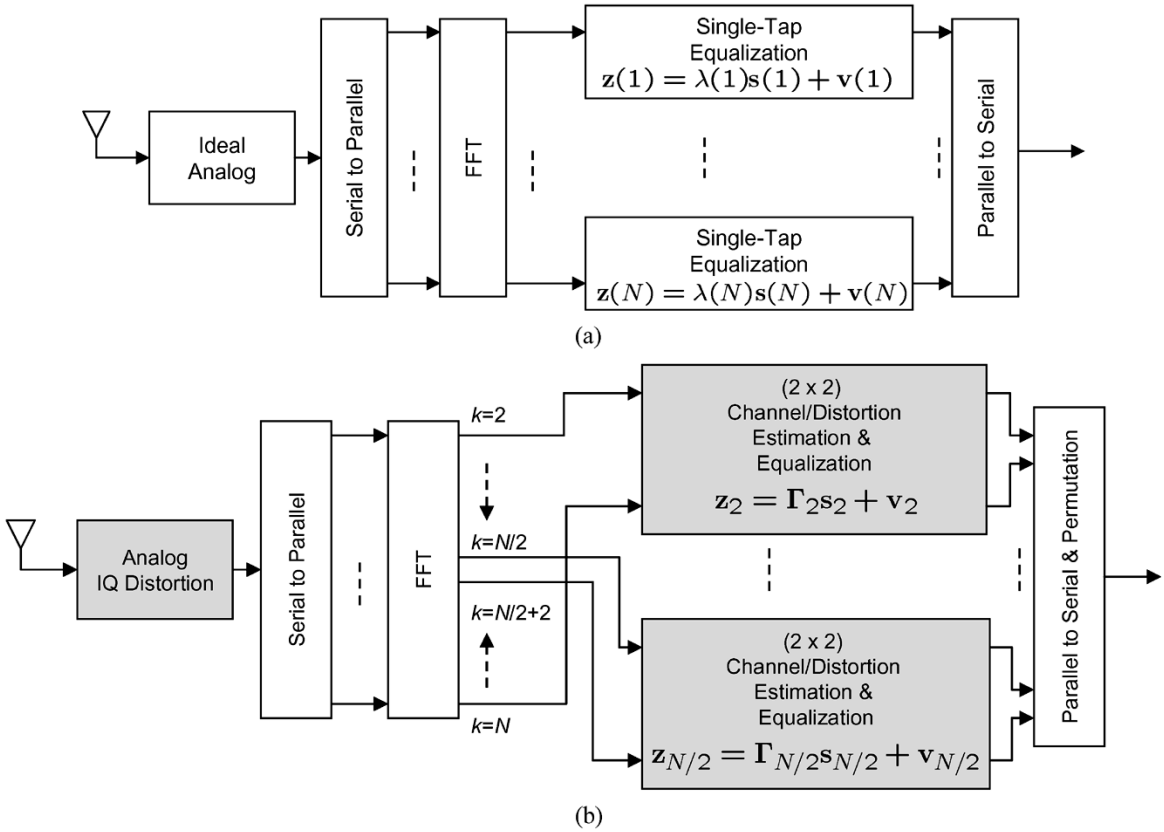

Fig. 5. Parameters inside the gray boxes ($\mathbf{z}_k, \mathbf{\Gamma}_k, \mathbf{s}_k$, and $\mathbf{v}_k$) are defined by (23) and (24). The estimation and equalization schemes are given in Section IV-A and B. The (2×2) set of equations in (b) reduce to decoupled scalar equations in (a) for a standard OFDM receiver with ideal IQ branches. (a) Standard OFDM receiver assuming *ideal* IQ branches. (b) OFDM receiver with post-FFT compensation of IQ *imbalances*.

receiver block diagram taking into account the IQ imbalances along with the compensation schemes described in this subsection and the following subsection is shown in Fig. 5(b). For comparison purposes, a standard OFDM receiver is also depicted in Fig. 5(a). Note that in a standard OFDM receiver, assuming ideal IQ imbalances, each gray box in Fig. 5(b) is substituted by two decoupled scalar equations, consequently requiring only scalar channel estimation and single-tap equalization. The standard receiver with ideal IQ branches is immediately obtained from (22)–(24) by substituting $\mu = 1$ and $\nu = 0$.

A performance analysis on the achievable SNR using this compensation scheme is now given and compared with that of a receiver with ideal IQ branches. Using (22) and the corresponding least-squares estimate given by (25), the error in the estimation of $\mathbf{s}_k$ is given by (assuming $\delta \approx 0$)

$$\tilde{\mathbf{s}}_k \stackrel{\Delta}{=} \hat{\mathbf{s}}_k - \mathbf{s}_k = \mathbf{\Gamma}_k^{-1}\mathbf{v}_k \tag{27}$$

and consequently, the covariance matrix of the error vector is

$$\mathbf{R}_{\tilde{\mathbf{s}}_k} \stackrel{\Delta}{=} \mathsf{E}(\tilde{\mathbf{s}}_k\tilde{\mathbf{s}}_k^*) = \sigma_v^2(\mathbf{\Gamma}_k^*\mathbf{\Gamma}_k)^{-1} \tag{28}$$

where $\mathbf{R}_{\mathbf{v}_k}$ was substituted by $\sigma_v^2\mathbf{I}_{2\times 2}$. Now, let us consider the $(1,1)$ element of $\mathbf{R}_{\tilde{\mathbf{s}}_k}$, which denotes the error variance in estimating $\mathbf{s}(k)$. It can be verified that

$$\mathbf{R}_{\tilde{\mathbf{s}}_k}(1,1) = \frac{\sigma_v^2}{|\lambda(k)|^2} \times \frac{|\mu|^2 + |\nu|^2}{|\mu^4| + |\nu^4| - 2|\mu^2\nu^2|}. \tag{29}$$

Note that the above expression collapses to

$$\frac{\sigma_v^2}{|\lambda(k)|^2} \tag{30}$$

for a receiver with ideal IQ branches ($\mu = 1$ and $\nu = 0$), as is expected. The difference between the error variance given by (29) for a receiver with least-squares equalization and the error variance given by (30) for a receiver with ideal IQ branches is defined as the loss in SNR (in decibels):

$$\text{Loss in SNR} = 10\log\left(\frac{|\mu|^2 + |\nu|^2}{|\mu^4| + |\nu^4| - 2|\mu^2\nu^2|}\right) \tag{31}$$

where μ and ν are related to the physical imbalances α and θ via (2). A similar expression can be derived for the error variance in estimating the other element of $\mathbf{s}_k$, namely, $\mathbf{s}(N-k+2)$. The above expression is plotted versus α and θ in the simulations section; see Fig. 12. For instance, the SNR degradation for reasonably large imbalances of phase (5°) and amplitude (1 dB) is lower bounded by 0.2 dB, which is an acceptable loss in SNR.

An adaptive implementation of the solution (25) is discussed next.

B. Adaptive Equalization

The adaptive estimation of $\mathbf{s}(k)$ and $\mathbf{s}^*(N-k+2)$ in (23) can be attained as follows:

$$\begin{aligned} \hat{\mathbf{s}}(k) &= \mathbf{w}_k\mathbf{z}_k \\ \hat{\mathbf{s}}^*(N-k+2) &= \mathbf{w}_{N-k+2}\mathbf{z}_k \end{aligned} \tag{32}$$

where $\mathbf{w}_k$ and $\mathbf{w}_{N-k+2}$ are 1×2 equalization vectors updated according to an adaptive algorithm (for instance LMS or some other adaptive form) for $k = \{2, \ldots, N/2\}$ [19]. To better illustrate the update equations, we introduce the time (or iteration) index i. As a result, let $\mathbf{w}_k^{(i)}$ and $\mathbf{w}_{N-k+2}^{(i)}$ represent the equalization vectors at time instant i. Furthermore, let $\mathbf{z}_k^{(i)}$ represent the vector $\mathbf{z}_k$ defined in (23) at time instant i. Now, the equalization coefficients for $k = \{2, \ldots, N/2\}$ are updated according to the LMS rules:

$$\mathbf{w}_k^{(i+1)} = \mathbf{w}_k^{(i)} + \mu_{\text{LMS}} \left(\mathbf{z}_k^{(i)}\right)^* e_k^{(i)} \tag{33}$$

$$\mathbf{w}_{N-k+2}^{(i+1)} = \mathbf{w}_{N-k+2}^{(i)} + \mu_{\text{LMS}} \left(\mathbf{z}_k^{(i)}\right)^* e_{N-k+2}^{(i)} \tag{34}$$

where $e_k^{(i)} = d_k^{(i)} - \mathbf{w}_k^{(i)} \mathbf{z}_k^{(i)}$ is the error signal generated at iteration i for the tone index k using a training symbol $d_k^{(i)}$, where the training symbol $d_k^{(i)}$ can be different for different tone indices k. A similar relation holds for $e_{N-k+2}^{(i)}$. Moreover, μ_{LMS} is the LMS step-size parameter.

Although LMS is the simplest adaptive implementation in terms of complexity, it suffers from a slow convergence rate [19]. This problem is severe for the application at hand since current OFDM systems usually deploy a short length for training symbols in order to reduce training overhead in packet-based data transmission. A short training length is acceptable due to the fact that an OFDM system with ideal I and Q branches can achieve a good channel estimation with only a few training symbols. This is achievable because in the case of ideal I and Q branches, the system of equations reduces to N decoupled equations, which result in an accurate estimate for the channel. However, in the presence of IQ imbalances, there is cross-coupling between every tone and its mirrored tone, which makes the convergence rate slower. In LMS, the coefficients in (33) and (34) are usually initiated with zero as their initial value. We propose a different initialization that enhances the convergence rate of the algorithm significantly. The equalizer coefficients are initialized to values calculated as if the receiver assumes ideal I and Q branches. This is how these initial values are calculated. Referring to (26) and setting $\mu = 1$ and $\nu = 0$, the system of equations for channel estimation becomes

$$\mathbf{z}_k = \begin{bmatrix} \mathbf{s}(k) & 0 \\ 0 & \mathbf{s}^*(N-k+2) \end{bmatrix} \begin{bmatrix} \lambda(k) \\ \lambda^*(N-k+2) \end{bmatrix} + \mathbf{v}_k. \tag{35}$$

Due to the diagonal structure of the above system, it can be seen that the least-squares solutions for $\lambda(k)$ and $\lambda^*(N-k+2)$ in (35) are given by [see also the notation defined in (23)]:

$$\hat{\lambda}(k) = \frac{\sum_{i=1}^{n_{\text{Tr}}} \mathbf{s}_i(k)^* \mathbf{z}_i(k)}{\sum_{i=1}^{n_{\text{Tr}}} \mathbf{s}_i(k)^* \mathbf{s}_i(k)} \tag{36}$$

where n_{Tr} is the number of training symbols. A new index i has been added to represent the symbol time instant. In other words, $\mathbf{s}_i(k)$ and $\mathbf{z}_i(k)$ are, respectively, the transmitted and received kth tones at time instant i. A similar expression holds for $\hat{\lambda}(N-k+2)$. Using the above estimation, which is derived assuming ideal IQ branches, the equalization vectors $\mathbf{w}_k$ and $\mathbf{w}_{N-k+2}$ in (32) are initialized to

$$\mathbf{w}_k^{(0)} = [\hat{\lambda}(k) \quad 0] \tag{37}$$

$$\mathbf{w}_{N-k+2}^{(0)} = [0 \quad \hat{\lambda}^*(N-k+2)]. \tag{38}$$

Using these initial values, (33) and (34) are then used to calculate the LMS solution. These calculated initial values are closer to the final value when compared with an all-zero initialization since the parameter ν in (24) is typically much smaller than the μ parameter. This algorithm is referred to as post-FFT LMS equalization.

C. Pre-FFT Distortion Correction With Channel Estimation

In the previous two subsections, the distortion due to IQ imbalance is estimated and compensated for after the FFT operation at the receiver, i.e., in the frequency domain. The correction and compensation can be performed before the FFT operation, i.e., in the time domain as well. In fact, a correction in time with the exact values of μ and ν can completely remove the distortion caused by IQ imbalance, as will be shown in this subsection.

Recalling (1) as the model for the distorted signal, it can be verified that

$$\begin{aligned} c(t) &\triangleq b'(t) - \left(\frac{\nu}{\mu^*}\right) b'^*(t) \\ &= \left(\mu - \frac{|\nu|^2}{\mu^*}\right) b(t). \end{aligned} \tag{39}$$

Therefore, the IQ distortion can be removed by using the above transformation given that the value of (ν/μ^*) is provided. Note that only the ratio between ν and μ^* is needed to calculate (39) and not the individual values. It is also seen from (39) that the SNR is preserved from $b(t)$ to $c(t)$. In other words, the IQ distortion can be removed, without degradation in SNR. This is only true for the noise added to the received signal before going through the IQ distortion. The noise added after the IQ distortion and before the correction given by (39) will be slightly enhanced, as is quantified below.

Let us assume perfect distortion parameters are available at the receiver. Now, we rewrite (1) and (39) as

$$b'(t) = \mu[b(t) + n_1(t)] + \nu[b(t) + n_1(t)]^* \tag{40}$$

$$c(t) = [b'(t) + n_2(t)] - \left(\frac{\nu}{\mu^*}\right) [b'(t) + n_2(t)]^* \tag{41}$$

where $n_1(t)$ is the noise added to the signal before being distorted by IQ imbalance, and $n_2(t)$ is the noise (assumed circular) added to the signal after the IQ distortion and before the correction given by (39). Then

$$\begin{aligned} c(t) = \underbrace{\left(\mu - \frac{|\nu|^2}{\mu^*}\right)}_{\rho} b(t) + \underbrace{\left(\mu - \frac{|\nu|^2}{\mu^*}\right)}_{\rho} n_1(t) \\ + n_2(t) - \left(\frac{\nu}{\mu^*}\right) n_2^*(t). \end{aligned} \tag{42}$$

Now, we calculate the SNR for the signal $c(t)$,

$$\text{Power of desired signal} = |\rho|^2\sigma_b^2 \tag{43}$$

$$\text{Noise contribution of } n_1 = |\rho|^2\sigma_{n_1}^2 \tag{44}$$

$$\text{Noise contribution of } n_2 = \underbrace{\left(1+\left|\frac{\nu}{\mu^*}\right|^2\right)}_{|\epsilon|^2}\sigma_{n_2}^2 \tag{45}$$

which results in the following expression for the SNR in the corrected signal $c(t)$:

$$\text{SNR}_{\text{corr. IQ}} = \frac{|\rho|^2\sigma_b^2}{|\rho|^2\sigma_{n_1}^2 + |\epsilon|^2\sigma_{n_2}^2} \tag{46}$$

which should be compared to the SNR if there were no IQ imbalance, given by

$$\text{SNR}_{\text{idealIQ}} = \frac{\sigma_b^2}{\sigma_{n_1}^2+\sigma_{n_2}^2}. \tag{47}$$

Therefore, the same SNR is preserved through the IQ correction process as if there was no IQ imbalance, only if the noise added to the signal after IQ distortion n_2 is assumed to be zero. Otherwise, there is a small loss in the final SNR, due to the IQ correction defined by (39). The loss in SNR is defined as

$$\begin{aligned}\text{Loss in SNR} &= 10\log\left(\frac{\text{SNR}_{\text{corr. IQ}}}{\text{SNR}_{\text{ideal IQ}}}\right)\\ &= 10\log\left(\frac{1+\frac{\sigma_{n_2}^2}{\sigma_{n_1}^2}}{1+\left|\frac{\epsilon^2}{\rho^2}\right|\frac{\sigma_{n_2}^2}{\sigma_{n_1}^2}}\right)\end{aligned} \tag{48}$$

which depends on the relative contribution of n_1 and n_2 in the overall receiver noise. This loss in dB is plotted in Fig. 13 for the case $\sigma_{n_2}^2/\sigma_{n_1}^2 = 1$.

Now, let us consider the problem of estimating the parameter (ν/μ^*) required for the operation defined by (39). Training sequences can be used to estimate this parameter. The channel estimates using the sets of equations defined by (26) can be used for (ν/μ^*) estimation: either the direct least-squares estimate or an adaptive implementation. Further, note that due to the structure of (26), it can be reduced to two decoupled sets of equations [using the definitions given by (23)]:

$$\mathbf{z}(k) = [\mathbf{s}(k) \quad \mathbf{s}^*(N-k+2)]\,[\,\mu\lambda(k)\nu\lambda^*(N-k+2)\,]+\mathbf{v}(k) \tag{49}$$

and

$$\begin{aligned}\mathbf{z}^*(N-k+2) = [\mathbf{s}(k) \quad \mathbf{s}^*(N-k+2)]\\ \times\begin{bmatrix}\nu^*\lambda(k)\\ \mu^*\lambda^*(N-k+2)\end{bmatrix}+\mathbf{v}(N-k+2).\end{aligned} \tag{50}$$

The above sets of equations can be used for estimating $\mu\lambda(k), \nu\lambda^*(N-k+2), \nu^*\lambda(k)$, and $\mu^*\lambda^*(N-k+2)$ in the least-squares sense; let us denote these quantities by $\hat{\rho}_1(k), \hat{\rho}_2(k), \hat{\rho}_3(k)$, and $\hat{\rho}_4(k)$, respectively. Now, two separate estimates for (ν/μ^*) for $k = \{2,\ldots,N/2\}$ can be obtained via

$$\left(\frac{\hat{\rho}_3(k)}{\hat{\rho}_1(k)}\right)^*, \left(\frac{\hat{\rho}_2(k)}{\hat{\rho}_4(k)}\right). \tag{51}$$

Assuming that the μ and ν parameters are constant over different tones $k = \{2,\ldots,N/2\}$, we can average the above estimates over all tones and select the result as an estimate for the parameter (ν/μ^*):

$$\widehat{\left(\frac{\nu}{\mu^*}\right)} = \frac{1}{N-2}\sum_{k=2}^{N/2}\left[\left(\frac{\hat{\rho}_3(k)}{\hat{\rho}_1(k)}\right)^* + \left(\frac{\hat{\rho}_2(k)}{\hat{\rho}_4(k)}\right)\right]. \tag{52}$$

Once the received signal is corrected before the FFT operation based on (39) and using the above estimate, a standard OFDM channel estimation and data decoding is conducted thereafter. The technique described here is referred to as pre-FFT correction with channel estimation.

The least-squares problem presented in this subsection needs to recover (51) from (49) and (50) by relying on two $(n_{\text{Tr}}\times 2)$ data matrices. The computational complexity and estimation performance can be improved by designing a specially patterned pilot sequence. Using this sequence, as described in the following subsection, the least-squares solution will rely on two data matrices that are $((n_{\text{Tr}}/2)\times 1)$ each.

D. Pre-FFT Distortion Correction With a Special Pilot Pattern

Recalling (49) and (50), the system of equations can be reduced from the vector-case to a scalar-case by transmitting zeros on tone $(N-k+2)$ during training, whereas known pilot values are transmitted on tone k; see Fig. 6. Using this pattern, (49) and (50) collapse to

$$\mathbf{z}(k) = \mathbf{s}(k)\underbrace{[\mu\lambda(k)]}_{\rho_1(k)}+\mathbf{v}(k) \tag{53}$$

and

$$\mathbf{z}^*(N-k+2) = \mathbf{s}(k)\underbrace{[\nu^*\lambda(k)]}_{\rho_3(k)}+\mathbf{v}(N-k+2) \tag{54}$$

Now, calculating the least-squares estimates of ρ_1 and ρ_3 assuming $(n_{\text{Tr}}/2)$ OFDM training symbols and substituting them into (51) results in the following estimate for $(\nu/\mu^*), k = \{2,\ldots,N/2\}$:

$$\left(\frac{\hat{\rho}_3(k)}{\hat{\rho}_1(k)}\right)^* = \left(\frac{\sum_{i=1}^{n_{\text{Tr}}/2}\mathbf{s}_i^*(k)\mathbf{z}_i(k)}{\sum_{i=1}^{n_{\text{Tr}}/2}\mathbf{s}_i^*(k)\mathbf{z}_i^*(N-k+2)}\right)^*. \tag{55}$$

A similar expression can be derived for the case that zeros are transmitted on tone k, and known pilot values are transmitted on tone $(N-k+2)$. Rewriting (53) and (54) for this case and deriving the least-squares estimates for $\rho_2(k)$ and $\rho_4(k)$ results in the following estimate for $(\nu/\mu^*), k = \{2,\ldots,N/2\}$

$$\left(\frac{\hat{\rho}_2(k)}{\hat{\rho}_4(k)}\right) = \frac{\sum_{i=1+n_{\text{Tr}}/2}^{n_{\text{Tr}}}\mathbf{s}_i(N-k+2)\mathbf{z}_i(k)}{\sum_{i=1+n_{\text{Tr}}/2}^{n_{\text{Tr}}}\mathbf{s}_i(N-k+2)\mathbf{z}_i^*(N-k+2)}. \tag{56}$$

The estimates from (55) and (56) are then averaged over different tones $k = \{2,\ldots,N/2\}$ in a similar manner to (52),

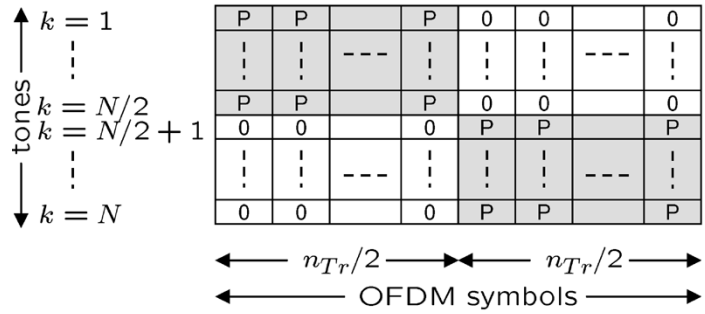

Fig. 6. Training scheme for both distortion and channel estimation. "P" stands for pilot sequence being transmitted, and "0" stands for no data being transmitted.

and the result chosen as an estimate for (ν/μ^*). As implicitly considered in (55) and (56), from a total of $n_{\rm Tr}$ training OFDM symbols, the first $(n_{\rm Tr}/2)$ training symbols only include pilot on tones $\{1,\ldots,N/2\}$ and zeros on the remaining tones, and the second $(n_{\rm Tr}/2)$ training symbols include pilot on tones $\{N/2+1,\ldots,N\}$ and zeros on the other tones. This switching is necessary since the training pilot tones have to include all the tones $\{1,\ldots,N\}$ in order to enable channel estimation on all the tones $\{\lambda(1),\ldots,\lambda(N)\}$. This training scheme is shown in Fig. 6. The compensation scheme proposed here is referred to as pre-FFT correction with a special pilot pattern.

E. Frequency-Flat versus Frequency-Selective Distortions

The distortion parameters μ and ν have been considered constant throughout the derivations, i.e., the parameters μ and ν defined by (2) were assumed to be frequency independent since the physical imbalances θ and α in (2) are considered to be so. An important consequence of this assumption is that the 2×2 channel matrices defined by (24) use the same μ and ν parameters for all the tones $k=\{2,\ldots,N/2\}$, i.e., μ and ν are independent of the tone index k. This is a valid assumption for OFDM systems such as IEEE802.11a that occupy a total bandwidth of less than 20 MHz. Experimental implementation of the analog processing over such bandwidths yields a frequency-flat IQ imbalance. However, for systems with higher bandwidths, this assumption is no longer realistic, and the imbalances may vary with frequency. Under such conditions, a frequency-selective IQ imbalance model should be used. For frequency-selective imbalances, the system of equations given by (22)–(24) can be modified by using frequency-dependent μ and ν parameters, i.e., by writing instead $\mu(k)$ and $\nu(k)$. This modification will not affect the post-FFT compensation schemes in Section IV-A and B since they did not use the k-independency of μ and ν. However, the pre-FFT compensation schemes in Section IV-C and D will be affected since a more sophisticated (higher order) time-domain distortion model (2), and consequently, a higher order pre-FFT compensation operation (39) is required. The frequency-selectivity of IQ imbalances highly depends on the ratio between the bandwidth and carrier frequency [6]. The higher this ratio, the more frequency-selective the imbalances will be. Therefore, for systems with relatively narrow bandwidth, the pre-FFT compensation schemes can be used. By using the pre-FFT compensation schemes, the operations performed after FFT will be the same as a standard

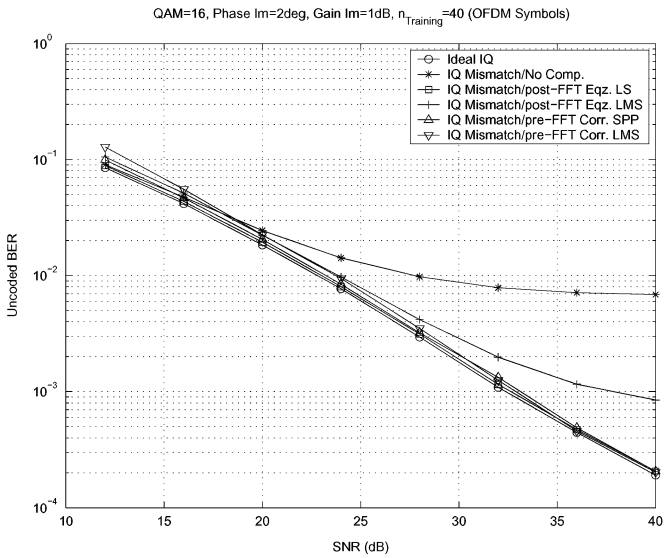

Fig. 7. BER versus SNR simulated for 16QAM constellation, phase imbalance of 2°, amplitude imbalance of 1 dB, and training length of 40 OFDM symbols.

OFDM receiver. Still, some processing is required to estimate the correction factor (ν/μ^*). Note that the post-FFT compensation schemes can be used as well. For systems with relatively wider bandwidth (compared to the carrier frequency), only the post-FFT compensation schemes presented in Section IV-A and B should be used since they can function for frequency-dependent distortion parameters μ and ν.

V. Simulation Results

A typical OFDM system is simulated to evaluate the performance of the proposed schemes in comparison to an ideal OFDM receiver with no IQ imbalance and a receiver with no compensation scheme. The parameters used in the simulation are OFDM symbol length of $N=64$, cyclic prefix of $P=16$, and channel length of $(L+1)=4$. The channel taps are chosen independently with complex Gaussian distribution. The BER versus SNR for the presented schemes are simulated and shown in Figs. 7–11. In all figures, "Ideal IQ" legend refers to a receiver with no IQ imbalance and perfect channel knowledge, and "IQ Mismatch/No Comp." refers to a receiver with IQ imbalance but no compensation scheme. "IQ Mismatch/post-FFT Eqz. LS," "IQ Mismatch/post-FFT Eqz. LMS," "IQ Mismatch/pre-FFT Corr. LMS," and "IQ Mismatch/pre-FFT Corr. SPP" refer to the

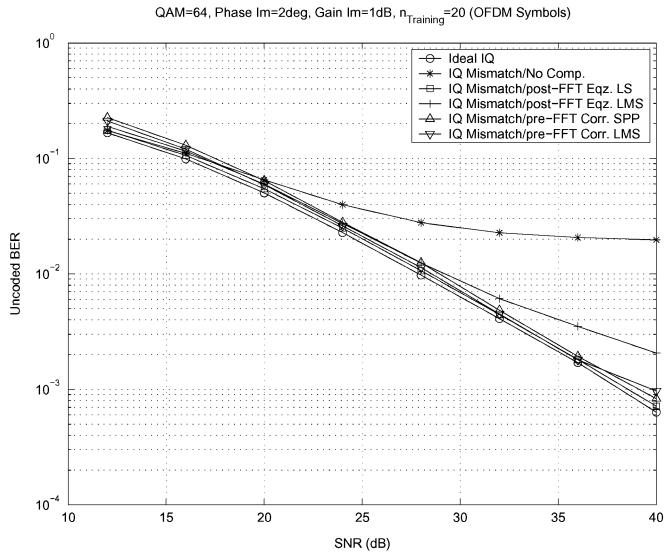

Fig. 8. BER versus SNR simulated for 64QAM constellation, phase imbalance of 2°, amplitude imbalance of 1 dB, and training length of 20 OFDM symbols.

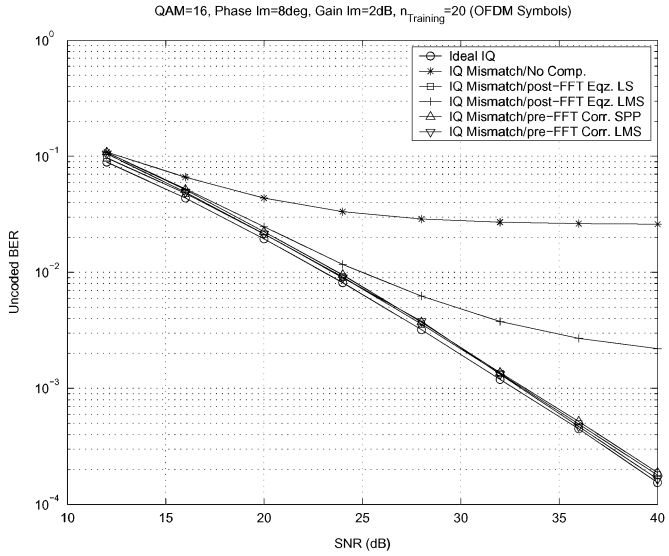

Fig. 9. BER versus SNR simulated for 16QAM constellation, phase imbalance of 8°, amplitude imbalance of 2 dB, and training length of 20 OFDM symbols.

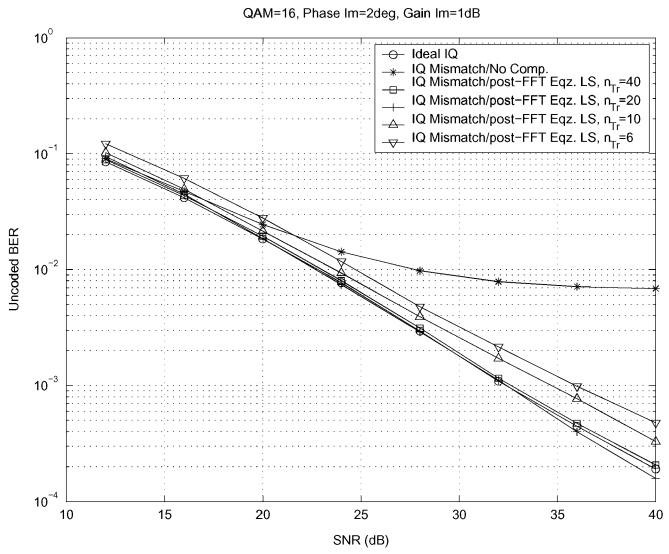

Fig. 10. BER versus SNR simulated for different lengths of training, plotted for post-FFT least-squares equalization (phase imbalance of 2° and amplitude imbalance of 1 dB).

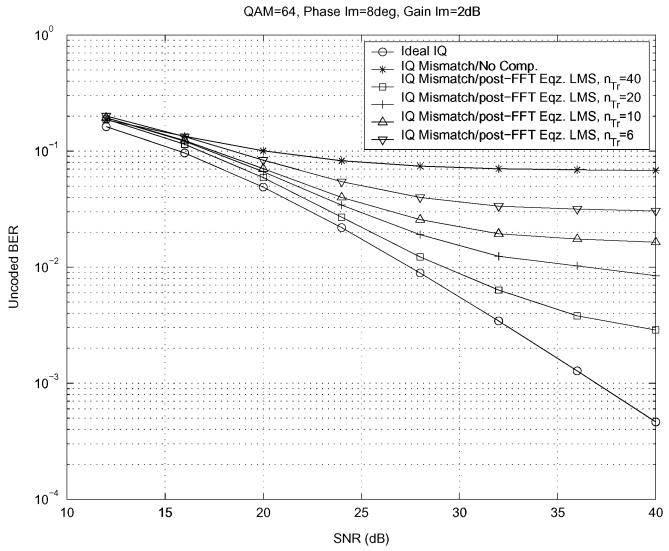

Fig. 11. BER versus SNR for different lengths of training, plotted for post-FFT adaptive equalization (LMS).

schemes presented in Section IV-A–D, respectively. The results are depicted for different constellation sizes (16 and 64QAM), different phase and amplitude IQ imbalances, and different lengths of training sequences. The LMS step-size parameter μ_{LMS} in Section IV-B was chosen to be 0.2 in the simulations.

As can be seen in all simulation results, the degradation in the BER values due to IQ imbalances is significant. Figs. 7–11 show the simulation results for typical (practical) distortion parameter values: phase and gain imbalances. An important observation is that the BER curves become saturated in the presence of IQ imbalances. In other words, even increasing the operating SNR does not help improve the BER values, emphasizing the need for compensation schemes. As was shown in Section IV, the loss in SNR due to IQ imbalances is small (less than 0.2 dB) when the least-squares compensation scheme is used. This can be seen in all simulation results where the BER curves for least-squares scheme almost coincide with the ideal case. The same results hold for the pre-FFT compensation schemes. It is shown that both the pre- and post-FFT (the least-squares scheme) algorithms perform very close to the ideal case. The results also show that the performance of the adaptive compensation scheme depends on the lengths of the available training sequence. The adaptive algorithm provides an acceptable BER when 20 OFDM symbols are available for training. Note that a decision directed approach can be used to provide that many number of training symbols in real scenarios.

Finally, Figs. 12 and 13 show the theoretical lower bounds on the loss in SNR due to IQ imbalances. The plots are based on the results derived in Section IV for both pre- and post-FFT compensation schemes. These bounds are calculated assuming

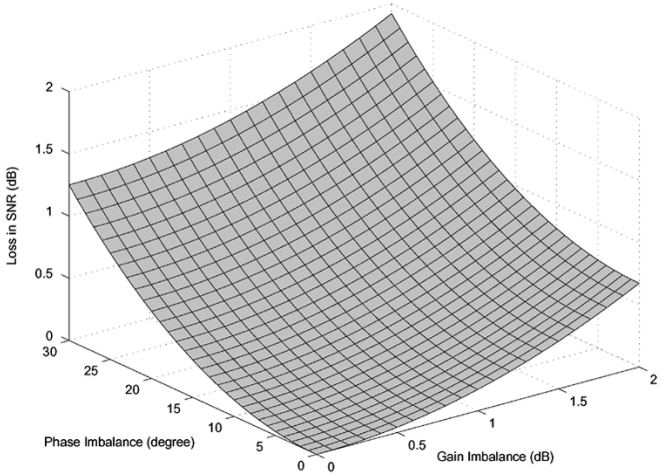

Fig. 12. Loss in SNR compared to the ideal IQ branches as a function of phase and amplitude imbalances when the post-FFT least-squares is applied as given by (31).

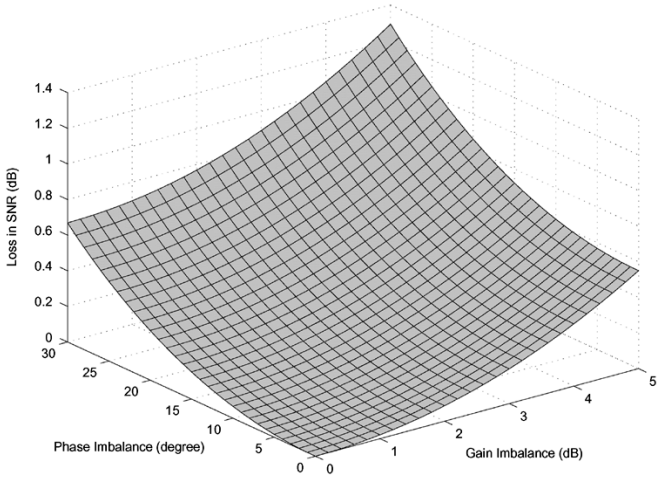

Fig. 13. Loss in SNR compared to the ideal IQ branches as a function of phase and amplitude imbalances when an ideal pre-FFT correction is applied. The derivation given by (48) and computed for the case $\sigma_{n_2}^2/\sigma_{n_1}^2 = 1$.

perfect channel and distortion parameter knowledge is available at the receiver, therefore serving as the theoretical lower bounds on the SNR loss due to imbalances.

VI. Conclusion

A framework for deriving OFDM receivers with IQ imbalance correction in the digital domain was presented. It was illustrated that the BER values for an OFDM system with typical IQ imbalances may be unacceptable. An important effect of IQ imbalances is that the achievable BER saturates as the SNR increases, suggesting that the system's performance at high SNR will be dominated by the IQ imbalances rather than the operating SNR. The performance degradation becomes more severe at high SNR values and high density transmit constellations. This highlights the need for compensation schemes for IQ imbalances. It was argued that compensation schemes developed in the analog domain may not be efficient in terms of power, area, and cost. Furthermore, such techniques in the analog domain cannot completely compensate for the distortions. The approach proposed in this paper relies on using signal processing techniques to compensate for analog domain impairments in the digital domain. There are several advantages associated with the proposed digital schemes, with the main advantage being that they allow us to exploit the digital processing power to alleviate problems arising from analog imperfections. Different algorithms to compensate for IQ distortions were developed and compared, namely, post-FFT equalization and pre-FFT correction schemes. The difference between frequency-flat and frequency-dependent IQ imbalance and its effect on the compensation scheme were discussed. It was shown that while the pre-FFT schemes function only for frequency-flat distortion, the post-FFT schemes can be used for both frequency-flat and frequency-selective distortions.

References

[1] *Part 11: Wireless LAN Medium Access Control (MAC) and Physical Layer (PHY) Specifications: High-Speed Physical Layer in the 5-GHz Band*, Dec. 1999. IEEE Std 802.11a-1999.

[2] *Part 11: Wireless LAN Medium Access Control (MAC) and Physical Layer (PHY) Specifications: Further Higher-Speed Physical Layer Extension in the 2.4 GHz Band*, 2003. IEEE Std 802.11g-2003.

[3] IEEE 802.15 Wireless Personal Area Networks (WPAN) High Rate Alternative PHY Task Group 3a (TG3a) [Online]. Available: http://www.ieee802.org/15/pub/TG3a

[4] IEEE 802.20 Mobile Broadband Wireless Access (MBWA) [Online]. Available: http://grouper.ieee.org/groups/802/20

[5] IEEE 802.16 Wireless Metropolitan Area Networks (WirelessMAN) [Online]. Available: http://www.wirelessman.org/

[6] B. Razavi, *RF Microelectronics*. Englewood Cliffs, NJ: Prentice-Hall, 1998.

[7] A. A. Abidi, "Direct-conversion radio transceivers for digital communications," *IEEE J. Solid-State Circuits*, vol. 30, no. 12, pp. 1399–1410, Dec. 1995.

[8] A. Tarighat and A. H. Sayed, "MIMO OFDM receivers for systems with IQ imbalances," *IEEE Trans. Signal Process.*, vol. 53, no. 9, Sep. 2005.

[9] A. Baier, "Quadrature mixer imbalances in digital TDMA mobile radio receivers," in *Proc. Int. Zurich Seminar Digital Commun., Electronic Circuits Syst. Commun.*, Zurich, Switzerland, Mar. 1990, pp. 147–162.

[10] C. L. Liu, "Impacts of I/Q imbalance on QPSK-OFDM-QAM detection," *IEEE Trans. Consum. Electron.*, vol. 44, no. 3, pp. 984–989, Aug. 1998.

[11] A. Schuchert, R. Hasholzner, and P. Antoine, "A novel IQ imbalance compensation scheme for the reception of OFDM signals," *IEEE Trans. Consum. Electron.*, vol. 47, no. 3, pp. 313–318, Aug. 2001.

[12] S. Fouladifard and H. Shafiee, "Frequency offset estimation in OFDM systems in presence of IQ imbalance," in *Proc. IEEE Int. Conf. Commun.*, vol. 3, Anchorage, AK, May 2003, pp. 2071–2075.

[13] J. Tubbax, B. Come, L. Van der Perre, S. Donnay, M. Engels, M. Moonen, and H. De Man, "Joint compensation of IQ imbalance and frequency offset in OFDM systems," in *Proc. Radio Wireless Conf.*, Boston, MA, Aug. 2003, pp. 39–42.

[14] A. Tarighat and A. H. Sayed, "On the baseband compensation of IQ imbalances in OFDM systems," in *Proc. IEEE Int. Conf. Acoust., Speech, Signal Process.*, vol. 4, Montreal, QC, Canada, May 2004, pp. 1021–1024.

[15] ——, "An optimum OFDM receiver exploiting cyclic prefix for improved data estimation," in *Proc. IEEE Int.Conf. Acoust., Speech, Signal Process.*, vol. 4, Hong Kong, Apr. 2003, pp. 217–220.

[16] Z. Pengfei, N. Thai, C. Lam, D. Gambetta, C. Soorapanth, C. Baohong, S. Hart, I. Sever, T. Bourdi, A. Tham, and B. Razavi, "A direct conversion CMOS transceiver for IEEE 802.11a WLANs," in *IEEE Int. Solid-State Circuits Conf. Dig. Technical Papers*, Feb. 2003.

[17] M. J. M. Pelgrom, A. C. J. Duinmaijer, and A. P. G. Welbers, "Matching properties of MOS transistors," *IEEE J. Solid-State Circuits*, vol. 24, no. 5, pp. 1433–1439, Oct. 1989.

[18] L. Der and B. Razavi, "A 2-GHz CMOS image-reject receiver with LMS calibration," *IEEE J. Solid-State Circuits*, vol. 38, no. 2, pp. 167–175, Feb. 2003.

[19] A. H. Sayed, *Fundamentals of Adaptive Filtering*. New York: Wiley, 2003.

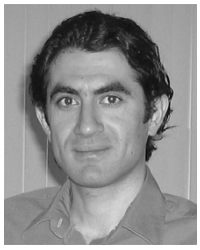

Alireza Tarighat (S'00) received the B.Sc. degree in electrical engineering from Sharif University of Technology, Tehran, Iran, in 1998 and the M.Sc. degree in electrical engineering from the University of California, Los Angeles (UCLA), in 2001, with emphasis on integrated circuits and systems. Since April 2002, he has been pursuing the Ph.D. degree in electrical engineering at UCLA.

During the summer of 2000, he was with Broadcom, El Segundo, CA, where he worked on designing IEEE 802.11a transceivers. From 2001 to 2002, he was with Innovics Wireless, Los Angeles, as a Senior Design Engineer, working on ASIC implementation of antenna diversity and rake processing for 3G WCDMA mobile terminals. His research focuses on signal processing techniques for communications, including MIMO OFDM receiver design and multiuser MIMO communications.

Mr. Tarighat received the Gold Medal of the National Physics Olympiad, Iran, in 1995 and the Honorable Mention Diploma of the 25th International Physics Olympiad, Beijing, China, in 1994.

Rahim Bagheri was born in Tehran, Iran, in 1975. He received the B.Sc. and M.Sc. degrees in electrical engineering, both with highest honor, from Sharif University of Technology, Tehran, in 1997 and 1999, respectively. He is currently pursuing the Ph.D. degree in electrical engineering at the University of California, Los Angeles, working on CMOS wireless transceiver circuits and architectures.

From 1999 to 2000, he was with UCLA MOSFET Research Lab, where he worked on sub 100-nm MOSFET design. He was with Valence Semiconductor Inc., Los Angeles, from 2000 to 2001 as a design engineer working on 802.11a CMOS radio. He was with JAALAA Inc., Los Angeles, in 2003 as an RFIC designer. He is co-founder of WiLinx Inc., Los Angeles, developing CMOS wireless communication chips.

Mr. Bagheri received the Gold Medal in National Physics Olympiad and Honorable Mention Diploma in the XXIV International Physics Olympiad in 2003. He received the Analog Devices Outstanding Student Designer Award in 2003 and UCLA Graduate Division Fellowship in 2000.

Ali H. Sayed (F'01) received the Ph.D. degree in electrical engineering in 1992 from Stanford University, Stanford, CA.

He is Professor and Chairman of electrical engineering at the University of California, Los Angeles. He is also the Principal Investigator of the UCLA Adaptive Systems Laboratory (www.ee.ucla.edu/asl). He has over 200 journal and conference publications, is the author of the textbook *Fundamentals of Adaptive Filtering* (New York: Wiley, 2003), is coauthor of the research monograph *Indefinite Quadratic Estimation and Control* (Philadelphia, PA: SIAM, 1999) and of the graduate-level textbook *Linear Estimation* (Englewood Cliffs, NJ: Prentice-Hall, 2000). He is also co-editor of the volume *Fast Reliable Algorithms for Matrices with Structure* (Philadelphia, PA: SIAM, 1999). He has contributed several articles to engineering and mathematical encyclopedias and handbooks and has served on the program committees of several international meetings. He has also consulted with industry in the areas of adaptive filtering, adaptive equalization, and echo cancellation. His research interests span several areas, including adaptive and statistical signal processing, filtering and estimation theories, signal processing for communications, interplays between signal processing and control methodologies, system theory, and fast algorithms for large-scale problems.

Dr. Sayed is recipient of the 1996 IEEE Donald G. Fink Award, a 2002 Best Paper Award from the IEEE Signal Processing Society, the 2003 Kuwait Prize in Basic Science, the 2005 Frederick E. Terman Award, and co-author of two Best Student Paper awards at international meetings. He is also a member of the technical committees on Signal Processing Theory and Methods (SPTM) and on Signal Processing for Communications (SPCOM), both of the IEEE Signal Processing Society. He is a member of the editorial board of the IEEE SIGNAL PROCESSING MAGAZINE. He has also served twice as Associate Editor of the IEEE TRANSACTIONS ON SIGNAL PROCESSING, of which he is now serving as Editor-in-Chief. He is serving as General Chairman of ICASSP 2008.